

## Turbulent transport mechanisms in Wendelstein 7-X plasmas

J.A. Alcusón<sup>1</sup>, F. Warmer<sup>1</sup>, P. Xanthopoulos<sup>1</sup>, O. Grulke<sup>1,2</sup> and the W7-X Team<sup>1</sup>.

<sup>1</sup> Max Planck Institut fuer Plasmaphysik, Greifswald, Germany

<sup>2</sup> Technical University of Denmark, Copenhagen, Denmark

**Introduction.** Radial transport in non-optimized stellarators is dominated by a high neo-classical (NC) contribution. In tokamaks, as this contribution is inherently minimal due to the symmetry of the device, the radial losses are essentially attributed to turbulence [1]. The optimized Wendelstein 7-X (W7-X) stellarator is designed to reduce the NC transport down to tokamak levels. Results from the first and the second experimental campaigns in W7-X suggest that NC transport is not sufficient to explain the radial losses in several scenarios (especially at the edge  $r_{eff} > 0.6$ ), opening the door to the turbulent transport contribution as a plausible candidate to explain these discrepancies.

The present work aims to serve as a guide for future studies connecting experimental and numerical estimations of turbulence in W7-X. Based on gyrokinetic simulations performed with the GENE code [2, 3] under W7-X experimental conditions, we will characterize the turbulent transport by identifying the dominant electrostatic instability (basically ion temperature gradient ITG, electron temperature gradient ETG and trapped-electron mode TEM) in two different configurations, standard (EIM) and high mirror (KJM), at ion scales (scales usually measured by the diagnostics). Simulations used in this analysis are linear, flux-tube and have kinetic ions and electrons. All simulations are set in the same magnetic surface<sup>1</sup> ( $s_0 = 0.5$ ). For each configuration two different scenarios are implemented: *core* and *edge*, both based on typical profiles measured during the last W7-X OP1.2a campaign.

<sup>1</sup>Instability growth rates also depend on the radial position, but in the profiles used for the study such variation is below 10% and the dominant instability is the same.

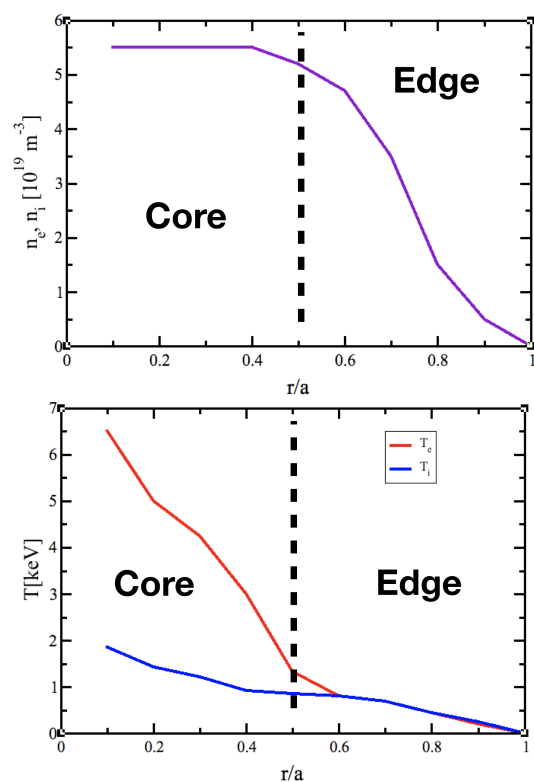


Figure 1: Profile examples for density (top) and temperatures (bottom) considered in GENE simulations.

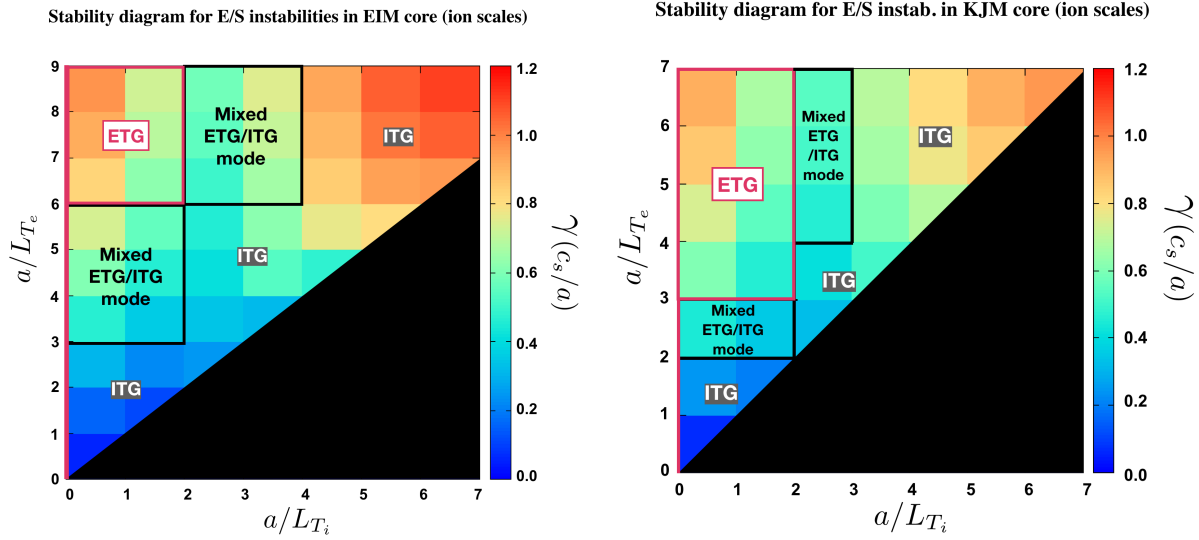


Figure 2: Stability maps in terms of  $a/L_{T_i}$  and  $a/L_{T_e}$  for core plasmas in standard (left) and high mirror (right) configurations. Dominant micro-instability regions at ion scale are also marked. The black region refers to not accessible conditions during OP1.2a.

Instabilities are characterized in terms of their propagation (ion or electron) direction and their mode amplitude structure (localized or extended). The dominant instability at ion scales is determined using a mixing length model in terms of  $\gamma / (k_y \rho)^2$ , where  $\gamma$  is the maximum growth rate of the instability, and  $k_y \rho$  the associated perpendicular wavenumber. A criteria where the ion scales are clearly favored.

**Stability maps.** In the core, W7-X density profiles are usually flat, but have a rather steep electron temperature ( $T_e$ ) profile (see Fig. 1). Therefore, our core simulations assume zero density gradients  $\nabla n = 0$ , and strong electron temperature gradients  $a/L_{T_e} \geq a/L_{T_i}$  where  $a$  is the minor radius and  $a/L_T = -a \nabla \ln T$ . The electron temperatures are usually higher than ion temperatures, so simulations are set for  $T_e/T_i = 3.5$ . Fig. 2 shows the stability map of the growth rates for both configurations. The ETG and ITG regions are slightly bigger in the high-mirror configuration reducing the "mixed mode" region, where the modes appear with similar growth rates at ion scales. In general both configuration exhibit a very similar map. The dominant instability switches from ITG to ETG (slab-style) as we increase the electron temperature gradient (from bottom to the top).

For the outer region of the plasma, our simulations assume coupled species:  $n_i = n_e$ ,  $T_i = T_e$  and  $\nabla T_e = \nabla T_i$  (see Fig 1). Fig. 3 shows stability maps in the outer plasma for both configurations. ITG and TEM regions similar to the standard configuration are also present in high mirror configuration. Nevertheless, strong gradients regions (top-right in the maps) show a dif-

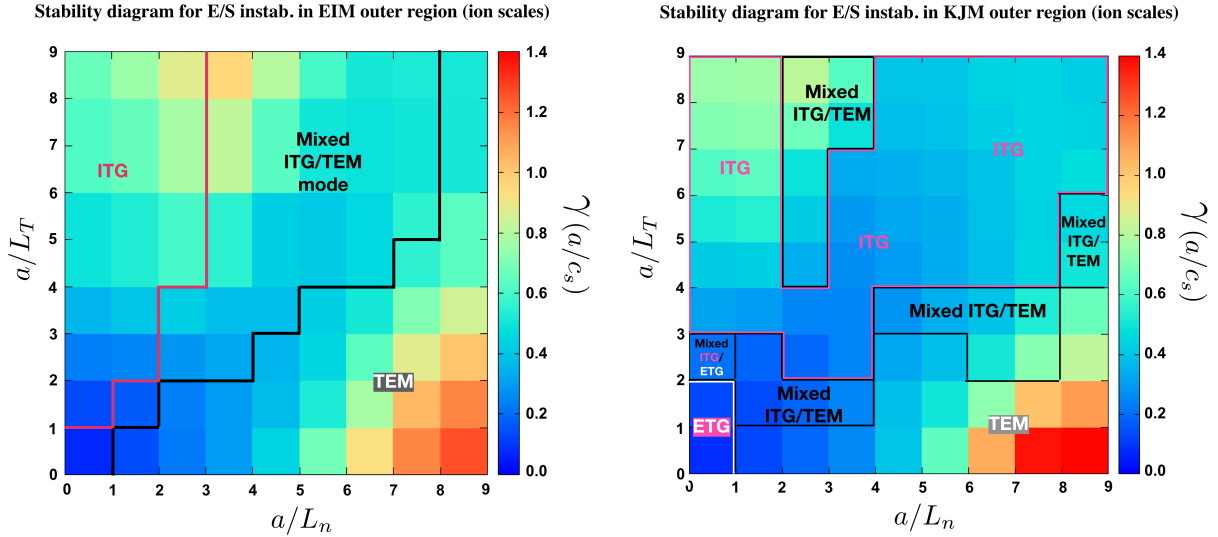


Figure 3: Stability maps in terms of  $a/L_n$  and  $a/L_T$  for core plasmas in standard (left) and high mirror (right) configurations. Dominant micro-instability regions at ion scale are also marked.

ferent behaviour. In fact, the high mirror configuration has a dominant ITG at ion scales and an ion driven TEM (iTEM) [5] instead of a mixed mode like in standard configuration as we can see in the left plot of Fig. 4. iTEM are trapped modes as the ordinary TEM, but propagate in the ion direction. They draw free energy from ions, rather than from electrons, but they need the trapped-electron population to exist and are associated to maximum-J configurations. By "mixed ITG/iTEM" instability we allude to a situation where the instabilities are practically indistinguishable regarding growth rates and scales. When both configurations exhibit the last mixed mode instability they usually have a similar growth rate, but the high mirror configuration has the instability displaced to shorter scales as we can see in the second plot of the same Fig. 4.

**Conclusions and future work.** Neoclassical transport estimations seem to have discrepancies with real measurements in the last W7-X campaigns and turbulent transport is the best candidate to explain these discrepancies. Stability maps are a very useful first step to characterize the dominant instability for future comparisons between turbulent transport experimental results and numerical simulations. Using general profiles from W7-X measured plasmas we can create these maps for different configurations. In particular, we show the stability maps of standard and high mirror configurations at ion scales. With the experimental profiles considered, only ITG and slab-ETG instabilities are possible in the core. These instabilities are not strongly influenced by the configuration, producing very similar stability maps for both cases.

In the outer plasma, ITG, TEM and slab-ETG instabilities can drive the turbulence at ion

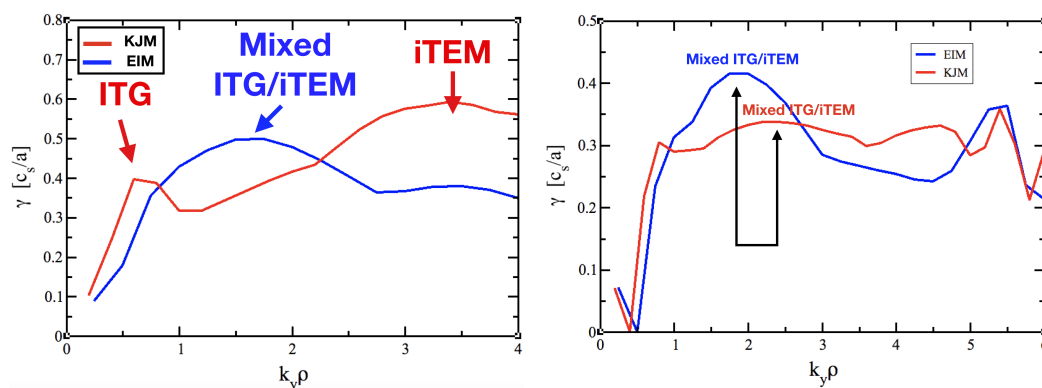


Figure 4: Left: Growth rate spectrum for standard (blue) and high mirror (red) configurations with  $a/L_n = 6$  and  $a/L_T = 8$ . Right: Same mixed ITG/iTEM instability for standard and high mirror.

scales. Stability maps are different in the strong gradient region, where the standard configuration exhibits a mixed ITG/iTEM instability whereas the high mirror configuration an ITG. In particular, the latter configuration also has a non dominant iTEM. Its higher quasi-isodynamicity than the standard configuration should reduce the trapped-electron population which probably is related with a weaker TEM response, allowing the ITG to become dominant. In the regions of mixed ITG/iTEM and of strong gradients, TEMs are not at the same scale, and usually high mirror TEMs are at smaller scales. The scale displacement implies different energy and fluxes in non-linear simulations even if both configurations have the same dominant instability and similar growth rate. Nonlinear simulations are also necessary to estimate the energy and fluxes produced by these instabilities. The ultimate goal is to quantify the total contribution of the turbulent transport to the power balance and clarify if the neoclassical estimations and turbulent contribution are enough to explain the heat losses.

## References

- [1] P. Helander, C.D. Beidler, T.M. Bird, M. Drevlak, Y. Feng, R. Hatzky, F. Jenko, R. Kleiber, J.H.E. Proll, Y. Turkin and P. Xanthopoulos, Phys. Control. Fusion **54**, 124009 (2012).
- [2] F. Jenko, W. Dorland, M. Kotschenreuther and B.N. Rogers, Phys. Plasmas **7**, 1904 (2000).
- [3] P. Xanthopoulos, H.E. Mynick, P. Helander, Y. Turkin, G.G. Plunk, F. Jenko, T. Goerler, D. Told, T. Bird and J.H.E. Proll, Phys. Rev. Lett. **113**, 155001 (2014).
- [4] J.H.E. Proll, P. Helander, J.W. Connor and G.G. Plunk, Phys. Rev. Lett. **108**, 245002 (2012).
- [5] G.G. Plunk, J.W. Connor and P. Helander, J. Plasma Phys. **83**, 715830404 (2017).